Polymer 257 (2022) 125260

Contents lists available at ScienceDirect

Polymer

journal homepage: www.elsevier.com/locate/polymer

Interchain ordering structure and main chain conformation analysis of thermal stability in vinyl-addition polynorbornene

Hideki Kai [a,*], Atsushi Izumi [b], Shun Hayakawa [c], J. Alex Niemiec [d,**], Carl Ebner [d], Mike Schofield [d], Doug Skilskyj [d], Larry F. Rhodes [d]

[a] Films & Sheets Research Laboratory, Sumitomo Bakelite Co., Ltd., 2-3-47 Higashi-Tsukaguchi-cho, Amagasaki, Hyogo, 661-8588, Japan
[b] Corporate Engineering Center, Sumitomo Bakelite Co., Ltd., 2100 Takayanagi, Fujieda, Shizuoka, 426-0041, Japan
[c] Advanced Materials Research Laboratory, Sumitomo Bakelite Co., Ltd., 20-7 Kiyohara Kogyodanchi, Utsunomiya, Tochigi, 321-3231, Japan
[d] Promerus LLC, 225 West Bartges Street, Akron, OH, 44307, USA

ARTICLE INFO

Keywords:
Vinyl-addition polynorbornene
Interchain ordering structure
Thermal stability

ABSTRACT

The aggregation structure and formation mechanism during film casting using toluene of vinyl-addition poly (norbornene-*co*-hexylnorbornene)s (P(NB/HNB)s) synthesized using Ni and Pd catalyst were systematically investigated by wide- and small-angle X-ray scattering and gel permeation chromatography–right-angle laser light scattering–viscometry techniques. The correlation of these data with the glass-transition temperature (T_g) was discussed. The single-chain conformation of P(NB/HNB)s was a flexible, stretched structure with respect to the Gaussian chain in a good solvent, as characterized by an exponent of the Mark–Houwink–Sakurada equation, and P(NB/HNB)s formed thin-rod aggregates with a length of 30 nm in semi-concentrated toluene solution via interchain stacking of the rod-like chains. P(NB/HNB) films cast from toluene solution exhibit interchain ordering structures with distances between 0.9 and 1.7 nm depending on the NB/HNB ratio. These findings show that the interchain ordering is driven by the stacking of the rod-like chains, which resulted in the highly ordered interchain structure in the film. The T_g of the Pd-catalyzed polymer films were 20 °C higher than that of the Ni-catalyzed polymer films depending on the interchain structure. There is a strong correlation between interchain ordering structure and T_g, which shows that the T_g of P(NB/HNB)s is primarily influenced by the van der Waals interaction between main chains.

1. Introduction

Norbornene can be converted into a thermoplastic amorphous polymer by ring-opening metathesis, vinyl-addition, cationic, and radical polymerization [1–7] In particular, vinyl-addition poly(norbornene) (PNB) shows high glass-transition temperature (T_g), low dielectric properties, high chemical resistance, and low water absorption, making them suitable for electronic applications [7–9]. However, PNB, having no side chain, is unsuitable for practical use because of its poor processability and mechanical brittleness [10]. As a result, various substituted PNB derivatives have been actively studied to improve the processability of film formation and the mechanical strength of films. Researchers at BFGoodrich demonstrated that incorporation of alkyl-2-norbornenes can help improve processability and can control the T_g by the length of the alkyl chains [11]. Kim et al. demonstrated that the T_g and mechanical properties of poly(norbornene-*co*-5--*n*-alkyl-2-norbornene) films can be tuned by controlling the amount of NB and the length of the *n*-alkyl chains [12]. The BFGoodrich researchers pointed out the need to lower T_g of the vinyl-addition PNB below its decomposition temperature in order to promote melt processing of this polymer. Wang et al. demonstrated that by introducing alkyl, aryl, and aryl ether groups to PNB, the temperature difference between T_g and the decomposition temperature can be increased by more than 100 °C [13]. As expected, these improvements in T_g were due to controlling the van der Waals interaction between PNB main chains, which was strongly correlated with interchain ordering and distance. To

* Corresponding author.
** Corresponding author.
E-mail addresses: h-kai@sumibe.co.jp (H. Kai), atsushi_i@sumibe.co.jp (A. Izumi), hayakawa-shun@sumibe.co.jp (S. Hayakawa), Alex.Niemiec@promerus.com (J.A. Niemiec), Carl.Ebner@Promerus.com (C. Ebner), Mike.Schofield@Promerus.com (M. Schofield), Doug.Skilskyj@promerus.com (D. Skilskyj), Larry.Rhodes@promerus.com (L.F. Rhodes).

https://doi.org/10.1016/j.polymer.2022.125260
Received 26 April 2022; Received in revised form 23 July 2022; Accepted 20 August 2022
Available online 24 August 2022

verify this conjecture, Ludovice and co-workers developed a rotational isomeric state model that includes long-range steric interactions and predicted that PNB adopts a unique helix–kink conformation [14–17]. This is one of the most important clues for elucidating the structural formation mechanism of interchain ordering, but no experimental studies have been performed to elucidate the formation mechanism and characterize the structure–thermal property relationship. In addition, the NMR pattern for the PNB without side chain reported to be different for Ni- and Pd-catalyzed P(NB/HNB)s [18,19], but the structural forming mechanism remain unexplored. These pioneering results for catalyst type should also be considered to elucidate interchain structure and mechanism of the substituted PNB derivatives in detail.

In this study, to characterize the structure–thermal property relationship of vinyl-addition PNB derivatives, aggregation structure and formation mechanism during film casting using toluene of poly(norbornene-*co*-hexylnorbornene)s (P(NB/HNB)s) with different NB/HNB ratios were investigated by wide- and small-angle X-ray scattering (WAXS and SAXS, respectively) and gel permeation chromatography (GPC)–right-angle laser light scattering (RALLS)–viscometry techniques. Here, two types of P(NB/HNB) synthesized using Ni and Pd catalyst were studied to be able to compare the differences in structure derived from the catalyst type. The correlation between aggregation structure and T_g of the cast films was systematically discussed.

2. Experimental

2.1. Materials

The Ni- and Pd-catalyzed vinyl-addition P(NB/HNB)s having NB/HNB ratios of 0/100, 50/50, and 80/20 (mol/mol) were provided by Promerus LLC (OH, USA) (Fig. 1). Vinyl addition P(NB/HNB)s were synthesized using a nickel and a palladium catalyst [18,20]. Ni-catalyzed vinyl addition P(NB/HNB)s were synthesized under an inert atmosphere in cyclohexane and ethyl acetate at 25–35 °C with a catalyst loading of 150–350:1 (mol monomer: mol catalyst). Monomer to solvent ratio ranged from 1:10 to 1:4. After 2 h, conversion was typically greater than 99%. Pd-catalyzed vinyl addition P(NB/HNB)s were synthesized under an inert atmosphere in toluene at 80 °C with catalyst loading of 25,000:1 (mol monomer: mol catalyst), co-catalyst loading of 2:1 (mol co-catalyst: mol catalyst), and 0.75 mol% chain transfer agent. Catalyst and co-catalyst delivery solvent was ethyl acetate. Monomer to solvent ratio was 1:4. After 2 h, conversion was typically greater than 99%. Their weight-average molecular weights (M_w) and polydispersity indices (PDI) are listed in Table 1, which were determined by GPC with polystyrene standards. GPC data were obtained by using a Tosoh EcoSEC HLC-8320GPC with a refractive index detector. The data were collected at 40 °C by using one PLgel 5 μm guard and two PLgel 5 μm Mixed-C columns with stabilized THF as the solvent. Polystyrene standards of known molecular weight were run by using the same conditions and column set to create a calibration curve. P(NB/HNB) films with a thickness of 0.1 mm were prepared by casting an 18 wt% P(NB/HNB) solution in toluene onto a polyethylene terephthalate substrate, followed by drying in a vacuum oven at 150 °C for 24 h.

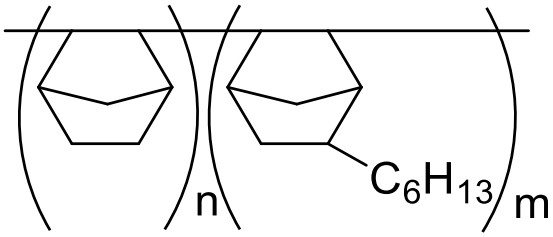

Fig. 1. Chemical structure of P(NB/HNB)s. n, and m show the repeat unit ratio of norbornene and hexylnorbornene, respectively.

Table 1
Weight-average molecular weight and polydispersity index.

	Ni		Pd	
NB/HNB (mol/mol)	M_w (g/mol)	PDI	M_w (g/mol)	PDI
0/100	147,000	1.98	177,000	3.16
50/50	191,000	2.41	168,000	3.91
80/20	171,000	3.16	146,000	4.01

2.2. WAXS and SAXS

WAXS and SAXS measurements were performed at the second hutch of the SPring-8 BL03XU beamline (Sayo, Hyogo, Japan) using a Pilatus 1M detector (DECTRIS Inc., Switzerland) [21,22]. WAXS measurements of the P(NB/HNB) films were performed over a q range of 2–20 nm^{-1} at a sample-to-detector distance (SDD) of 0.3 m and an incident X-ray wavelength (λ) of 0.10 nm. Here, q represents the magnitude of the scattering vector given by $q = (4\pi/\lambda)\sin(2\theta/2)$, where 2θ denotes the scattering angle. SAXS measurements of 3 wt% P(NB/HNB) solutions in toluene were performed over a q range of 0.05–7 nm^{-1} at three SDDs of 4.3, 1.7, and 0.6 m and with a λ of 0.10 nm using a 2-mm solution cell sealed with two 0.03 mm-thick glass plates. All measurements were performed at room temperature.

2.3. GPC–RALLS–viscometry

GPC analyses for the evaluation of intrinsic viscosity ([η]) in THF as a function of absolute molecular weight (M) were performed on an AT-2002 system (Asahi Techneion Co., Ltd., Japan) equipped with three poly(styrene-co-divinylbenzene) gel columns TSKgel G100H_{HR}, G2500H_{HR}, and G4000H_{HR} (Tosoh Corporation, Japan) and a triple detector array Viscotek TDA 302 (Malvern Panalytical Ltd., U.K.). The absolute molecular weight and intrinsic viscosity were measured by a RALLS detector with a laser light wavelength of 670 nm and a four-capillary differential viscometer, respectively. THF at 40 °C was used as the eluent, and the polymer concentration of the injection solution was 0.2 wt%. Mark–Houwink–Sakurada (MHS) analysis was conducted at a nearly theta condition for the investigated PNBs [23,24].

2.4. DMA

A dynamic mechanical analysis (DMA) was performed on a dynamic mechanical analyzer (DMA Q800) (TA Instruments Inc., TX, USA) to determine the thermal properties of the P(NB/HNB) films. The length and width of the specimen were 35 and 8 mm, respectively, and the thickness of the rectangular film was 0.10 mm. The DMA measurement was performed from 25 °C to 320 °C at a ramp rate of 5 °C/min under a nitrogen atmosphere in a multi-frequency-strain temperature ramp mode with 1 Hz frequency, 0.1% strain, and 0.001 N preload force.

3. Results and discussion

WAXS profiles of the P(NB/HNB) films are shown in Fig. 2. All WAXS profiles show two primary peaks corresponding to interchain ordering at a lower q region from 2 to 10 nm^{-1} and amorphous structure at a higher q region from 10 to 20 nm^{-1}, as reported in previous studies [12,25,26]. The peak at a higher q region corresponds to a short-range carbon–carbon correlation in the amorphous polymer structure, and the peak top q value (q_2) of 13.4 nm^{-1} shows the correlation distance in real space (d-spacing) was 0.47 nm, which was calculated by $2\pi/q_2$ and the d-spacing was summarized in Table 2. The peak top position q_2 is constant regardless of the NB/HNB ratio and catalyst type, showing that all polymer chains exhibit a similar amorphous structure in the film. The peak at a lower q region corresponds to the distance of interchain

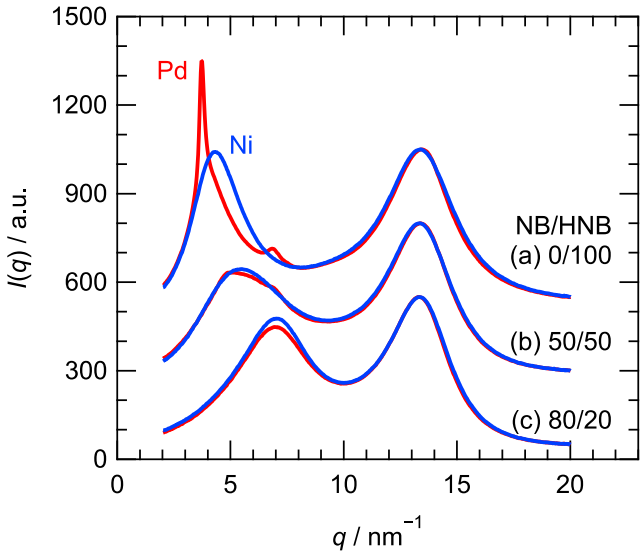

Fig. 2. WAXS profiles of P(NB/HNB) films with the NB/HNB ratios of (a) 0/100, (b) 50/50, and (c) 80/20. Red and blue lines represent P(NB/HNB) synthesized using Ni and Pd catalyst, respectively. For clarity, profiles (a) and (b) are vertically shifted by 300 each. (For interpretation of the references to colour in this figure legend, the reader is referred to the Web version of this article.)

Table 2
WAXS Peak top *d*-spacing of P(NB/HNB) films.

	d-spacing at q_1 (nm)		*d*-spacing at q_2 (nm)	
NB/HNB ratio (mol/mol)	Ni	Pd	Ni	Pd
0/100	1.44	1.69	0.47	0.47
50/50	1.16	1.27	0.47	0.47
80/20	0.89	0.90	0.47	0.47

ordering between polymer chains, and the peak top q value (q_1) shifted to the lower q region as the NB/HNB ratio decreased regardless of the catalyst type, which shows that the steric hindrance of the hexyl side chain increased the average distance of the interchain ordering. The side chain effect on the interchain distance was not a unique behavior for our system but was also observed for poly(norbornene-*co*-octylnorbornene)s prepared by a Pd catalyst [12]. Here, the peak shape of the interchain ordering of the 0/100 polymers was clearly different between Ni and Pd catalyst. The narrow peak of Pd shows that the interchain distance of Pd-catalyzed P(NB/HNB)s was more ordered than that of Ni, which suggests that Pd-catalyzed P(NB/HNB)s exhibit higher stereoregularity of the polymer chain compared to Ni-catalyzed P(NB/HNB)s. The peak shape of Pd-catalyzed P(NB/HNB)s became broader as the NB/HNB ratio increased, which was because the introduction of the NB units decreased the stereoregularity of the primary chain due to the HNB units. In addition to the major two peaks of the interchain ordering and amorphous structures, a small peak can be observed at 6.9 nm^{-1} in the WAXS profiles of Pd-catalyzed- P(NB/HNB)s with the NB/HNB ratios of 0/100 and 50/50. Although the structure that gave this peak corresponding to the *d*-spacing of 0.92 nm is not clear at this moment, the presence of this peak is another result that supports the higher stereoregularity of the Pd-catalyzed- P(NB/HNB)s.

The driving force of the interchain ordering of PNBs is thought to be stacking of the rod-like main chain. However, there have been few studies that discuss the rod-like structure in detail based on experimental results. A single-chain conformation in solution can be evaluated by an exponent (a) of the Mark–Houwink–Sakurada (MHS) equation given by $[\eta] = KM^a$, where K denotes a constant that depends on polymer, solvent, temperature, and so on. The exponent a is 0.5 when a polymer behaves like a Gaussian chain in solution. The value becomes larger than 0.5 when the polymer conformation is stretched compared to the Gaussian chain. Ahmed et al. investigated the MHS analysis for poly(norbornene) and poly(butylnorbornene) and determined the value a was 1.9 in a theta condition [16]. Although the exponent 2 is a value for an absolute rigid rod structure such as tobacco mosaic virus, they recognized that the value was subject to considerable error. They concluded that a value greater than 0.5 supported the helix–kink conformation of PNB predicted by an atomistic simulation. To determine the exponent more precisely, a careful evaluation of the intrinsic viscosity's absolute molecular weight dependence is required, and the GPC-based comprehensive approach using a light scattering detector and viscometer is a powerful technique for addressing this issue. The MHS plot obtained by the GPC–RALLS–viscometry in THF at 40 °C is shown in Fig. 3. All polymers exhibit exponents a of 0.6–0.7 in THF. A value greater than 0.5 in comparison to the Gaussian chain shows that all polymers have a flexible, stretched conformation, implying that the interchain ordering is driven by the stacking of rod-like chains. There was no difference in the a values between investigated polymers; however, the values $[\eta]$ of Pd-catalyzed P(NB/HNB)s were greater than those of Ni-catalyzed P(NB/HNB)s in the investigated molecular weight range, irrespective of the NB/HNB ratio. Additionally, the difference in $[\eta]$ between Pd- and Ni-catalyzed P(NB/HNB)s became larger as the NB/HNB ratio decreased. This specific behavior of $[\eta]$ for P(NB/HNB)s is an important clue for delving deeper into the conformation of PNB. As previously stated, Ludovice and co-workers proposed that PNBs adopt a helix–kink conformation [14–17]. Assuming that P(NB/HNB)s also adopt the helix–kink conformation, the Pd-catalyzed P(NB/HNB)s with a higher $[\eta]$ have fewer kinks in the main chain than the Ni-catalyzed P(NB/HNB)s, because the kink structure in the main chain effectively lowers $[\eta]$ by decreasing the stereoregularity of the main chain. The kink-less, rod-like main chain structure of the Pd-catalyzed P(NB/HNB), that was characterized by the higher $[\eta]$, may allow effective stacking and a highly ordered aggregated structure, which correlates with the result that the Pd-catalyzed P(NB/HNB) film has a sharper peak than the Ni-catalyzed P(NB/HNB) film in the (a) 0/100 WAXS profile in Fig. 2. A decrease in the $[\eta]$ difference between Pd- and Ni-catalyzed P(NB/HNB)s was observed with an increase in the NB/HNB ratio. This phenomenon

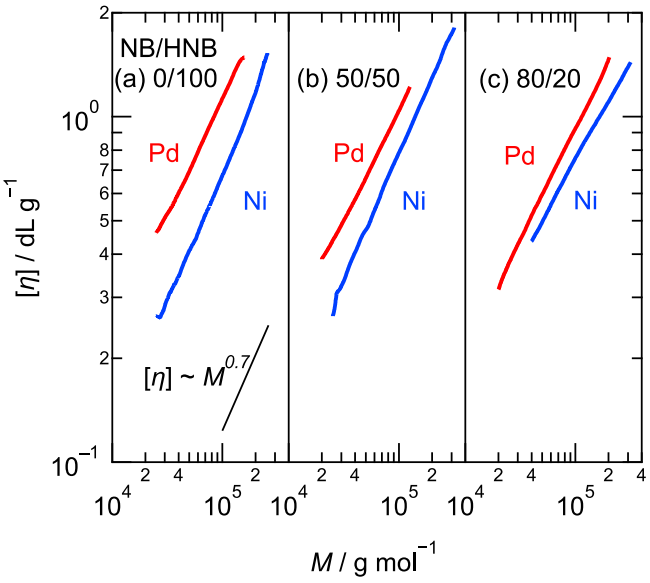

Fig. 3. Mark–Houwink–Sakurada plot in THF of P(NB/HNB) with the NB/HNB ratios of (a) 0/100, (b) 50/50, and (c) 80/20. Red and blue lines represent P(NB/HNB) synthesized using Ni and Pd catalyst, respectively. (For interpretation of the references to colour in this figure legend, the reader is referred to the Web version of this article.)

can be attributed to random copolymerization that decreased the stereoregularity of the main chain, and the decrease in the stereoregularity caused broadening of the WAXS peak shape of Pd-catalyzed P(NB/HNB)s with an increase in the NB/HNB ratio.

The exponent of the MHS equation in a dilute THF solution provides information about the single-chain conformation. To elucidate the main chain aggregation behavior during the film forming process in more detail, structure analysis in semi-concentrated solution in toluene was performed by SAXS. The SAXS profiles of the 3 wt% solution are shown in Fig. 4, in which the scattering of toluene was subtracted as background. Each sample shows a characteristic behavior that obeys a power low relation of $I(q) \sim q^{-1}$ in a wide q range, in which $I(q)$ denotes scattering intensity. The exponent -1 denotes a structure of thin-rod aggregation. The -1 power increased to 0.2 nm^{-1} in the lower q region, showing that the length of the thin-rod aggregate was 30 nm. A clear peak was observed at 2–6 nm^{-1} for both (a) 0/100 and (b) 50/50. The presence of the peak shows that the interchain ordered aggregation, which was confirmed by WAXS profile of the film in Fig. 2, was already formed in the semi-concentrated solution; that is, the single chain of P(NB/HNB)s has a rod-like conformation, and thin-rod aggregates are formed by stacking the rod-like single chains in a semi-concentrated regime. This aggregation formation mechanism during film casting using toluene was enhanced during the drying process, which resulted in the formation of the highly ordered interchain stacked structure in the film.

BFGoodrich researchers reported that increasing the copolymerization ratio of alkylnorbornene to norbornene decreases the T_g of the copolymer film [11]. This is because the van der Waals interaction between chains decreases with increasing the interchain ordering distance. In addition to these typical copolymerization ratio trends, the main chain conformation is expected to influence the interchain van der Waals interaction between chains and the thermal properties of P(NB/HNB)s. The T_g of P(NB/HNB) films was investigated by DMA to characterize the interchain ordering structure–thermal property relationship. The temperature dependence of the storage modulus of P(NB/HNB) films is shown in Fig. 5. The T_g was determined by the DMA curve's inflection point for the storage modulus. As with all films, both the T_g and the storage modulus increased with the NB/HNB ratio, which

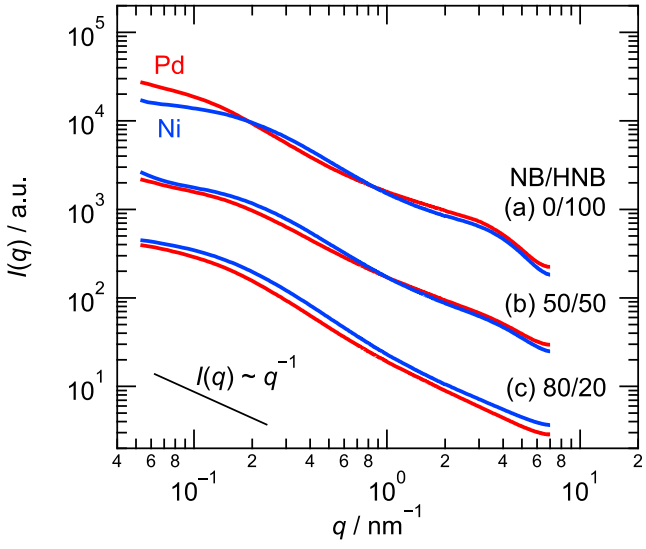

Fig. 4. SAXS profiles of 3 wt% toluene solution of P(NB/HNB) with NB/HNB ratios of (a) 0/100, (b) 50/50, and (c) 80/20. Red and blue lines represent P(NB/HNB) synthesized using Ni and Pd catalyst, respectively. For clarity, profiles (a) and (b) are vertically shifted by a factor of 10 each. (For interpretation of the references to colour in this figure legend, the reader is referred to the Web version of this article.)

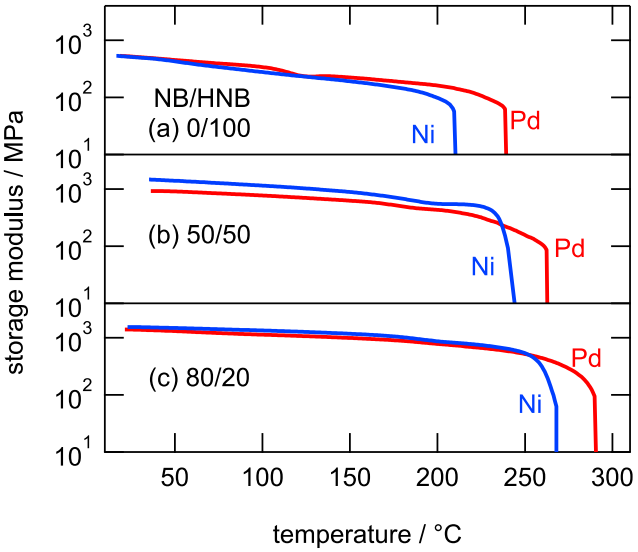

Fig. 5. Temperature dependence of storage modulus on P(NB/HNB) films with the NB/HNB ratios of (a) 0/100, (b) 50/50, and (c) 80/20. Red and blue lines represent P(NB/HNB) synthesized using Ni and Pd catalyst, respectively. (For interpretation of the references to colour in this figure legend, the reader is referred to the Web version of this article.)

was due to a decrease in the steric hindrance between main chains, which agrees with previous studies [12]. In contrast to these typical trends, the catalyst types varied the T_g values significantly, while little impact was observed in the storage modulus below 200 °C; the T_g of the Pd-catalyzed P(NB/HNB) film was 20 °C higher than that of the Ni-catalyzed P(NB/HNB) film, regardless of the NB/HNB ratio. This supports the hypothesis that the film's T_g was affected not only by the NB/HNB ratio but also by the kink structure in the main chain, as shown by the difference in $[\eta]$.

4. Conclusions

We investigated the nano-scaled aggregation structure and its formation mechanism during film casting using toluene of vinyl-addition P(NB/HNB)s by WAXS, SAXS, and GPC–RALLS–viscometry techniques to explain its correlation with the T_g of the cast film. All polymers have interchain ordering structures with distances between 0.9 and 1.7 nm depending on the NB/HNB ratio. The exponent of the MHS equation showed that the single-chain conformation of P(NB/HNB)s was flexible, stretched in relation to the Gaussian chain in a good solvent, and P(NB/HNB)s aggregated into thin-rod with a length of 30 nm in semi-concentrated toluene solution. These findings show that the interchain ordering is driven by the stacking of the rod-like chains, which resulted in the highly ordered interchain structure in the film. Additionally, the Pd-catalyzed P(NB/HNB)s showed a kink-less structure in the main chain when compared to the Ni-catalyzed P(NB/HNB)s, which was characterized by a higher $[\eta]$, and the kink-less structure increased the interchain ordering and T_g. The clear relationship between the interchain ordering structure and the T_g of P(NB/HNB)s was characterized through experimental elucidation of the interchain ordering structure and its formation mechanism during film casting using toluene. We believe that detail NMR analyses focusing on the kinks will also provide information on the formation of the kinks. As for polymer synthesis research, clarification of the origin of different chain structures including thermodynamics in catalytic cycles is an important issue and is our future challenge.

CRediT authorship contribution statement

Hideki Kai : Conceptualization, Methodology, Investigation, Writing – original draft.

Atsushi Izumi : Conceptualization, Methodology, Investigation, Writing – original draft.

Shun Hayakawa : Resources.

J. Alex Niemiec : Resources, Writing – review & editing.

Carl Ebner : Resources.

Mike Schofield : Resources.

Doug Skilskyj : Resources.

Larry F. Rhodes : Resources, Writing – review & editing.

Declaration of competing interest

The authors declare that they have no known competing financial interests or personal relationships that could have appeared to influence the work reported in this paper.

Data availability

No data was used for the research described in the article.

Acknowledgment

The WAXS and SAXS experiments were performed at SPring-8 BL03XU beamline (FSBL) with the approval of the Japan Synchrotron Radiation Research Institute (proposal numbers 2021A7208, 2021B7258, and 2022A7209).

References

[1] K.J. Ivin, J.C. Mol, Olefin Metathesis and Metathesis Polymerization, second ed., Academic Press, San Diego, 1997.

[2] J.P. Kennedy, H.S. Makowski, Carbonium ion polymerization of norbornene and its derivatives, J. Macromol. Sci., Chem. A. 1 (1967) 345–370, https://doi.org/10.1080/10601326708053976.

[3] N.G. Gaylord, A.B. Deshpande, Structure of "vinyl-type" polynorbornenes prepared with ziegler-natta catalysts, J. Polym. Sci., Polym. Lett. Ed. 14 (1976) 613–617, https://doi.org/10.1002/pol.1976.130141007.

[4] N.G. Gaylord, B.M. Mandal, M. Martan, Peroxide-induced polymerization of norbornene, J. Polym. Sci., Polym. Lett. Ed. 14 (1976) 555–559, https://doi.org/10.1002/pol.1976.130140908.

[5] N.G. Gaylord, A.B. Deshpande, B.M. Mandal, M. Martan, Poly-2,3- and 2,7-bicyclo [2.2.1]hept-2-enes: preparation and structures of polynorbornenes, J. Macromol. Sci., Chem. 11 (1977) 1053–1070, https://doi.org/10.1080/00222337708061307.

[6] F. Blank, C. Janiak, Metal catalysts for the vinyl/addition polymerization of norbornene, Coord. Chem. Rev. 253 (2009) 827–861, https://doi.org/10.1016/j.ccr.2008.05.010.

[7] C. Janiak, P.G. Lassahn, Metal catalysts for the vinyl polymerization of norbornene, J. Mol. Catal. Chem. 166 (2001) 193–209, https://doi.org/10.1016/S1381-1169(00)00475-1.

[8] M.V. Bermeshev, P.P. Chapala, Addition polymerization of functionalized norbornenes as a powerfultool for assembling molecular moieties of new polymers withversatile properties, Prog. Polym. Sci. 84 (2018) 1–46, https://doi.org/10.1016/j.progpolymsci.2018.06.003.

[9] G.O. Karpov, D.A. Alentiev, A.I. Wozniak, E.V. Bermesheva, I.V. Lounev, Y. A. Gusev, V.P. Shantarovich, M.V. Bermeshev, Dielectric properties of addition and metathesis polynorbornenes with bulky side-substituents, Polymer 203 (2020), 122759, https://doi.org/10.1016/j.polymer.2020.122759.

[10] N.R. Grove, P.A. Kohl, S.A.B. Allen, S. Jayaraman, R. Shick, Functionalized polynorbornene dielectric polymers: adhesion and mechanical properties, J. Polym. Sci. B Polym. Phys. 37 (1999) 3003–3010, https://doi.org/10.1002/(SICI)1099-0488(19991101)37:21<3003::AID-POLB10>3.0.CO;2-T.

[11] B.L. Goodall, G.M. Benedikt, L.H. McIntosh, D.A. Barnes, The B.F. Goodrich Company, Process for making polymers containing a norbornene repeating unit by addition polymerization using an organo (nickel or palladium) complex, U.S. Patent 5 (Nov. 21, 1995), 468,819.

[12] E.C. Kim, M.J. Kim, L.N. Thi Ho, W. Lee, J.W. Ka, D.G. Kim, T.J. Shin, K.M. Huh, S. Park, Y.S. Kim, Synthesis of vinyl-addition polynorbornene copolymers bearing pendant *n*-alkyl chains and systematic investigation of their properties, Macromolecules 54 (2021) 6762–6771, https://doi.org/10.1021/acs.macromol.1c00858.

[13] X. Wang, Y.L. Jeong, C. Love, H.A. Stretz, G.E. Stein, B.K. Long, Design, synthesis, and characterization of vinyl-addition polynorbornenes with tunable thermal properties, Polym. Chem. 12 (2021) 5831–5841, https://doi.org/10.1039/d1py01050f.

[14] S. Ahmed, S.A. Bidstrup, P. Kohl, P. Ludovice, Stereochemical structure-property relationships in polynorbornene from simulation, Macromol. Symp. 133 (1998) 1–10.

[15] S. Ahmed, S.A. Bidstrup, P.A. Kohl, P.J. Ludovice, Development of a new force field for polynorbornene, J. Phys. Chem. B 102 (1998) 9783–9790, https://doi.org/10.1021/jp9814294.

[16] S. Ahmed, P.J. Ludovice, P. Kohl, Microstructure of 2,3 erythro di-isotactic polynorbornene from atomistic simulation, Comput. Theor. Chem. 10 (2000) 221–233, https://doi.org/10.1016/S1089-3156(99)00083-5.

[17] W.J. Chung, C.L. Henderson, P.J. Ludovice, RIS model of the helix-kink conformation of erythro diisotactic polynobornene, Macromol. Theory Simul. 19 (2010) 421–431, https://doi.org/10.1002/mats.201000003.

[18] D.A. Barnes, G.M. Benedikt, B.L. Goodall, S.S. Huang, H.A. Kalamarides, S. Lenhard, L.H. McIntosh, K.T. Selvy, R.A. Shick, L.F. Rhodes, Addition polymerization of norbornene-type monomers using neutral nickel complexes containing fluorinated aryl ligands, Macromolecules 36 (2003) 2623–2632, https://doi.org/10.1021/ma030001m.

[19] B.L. Goodall, Cycloaliphatic polymers via late transition metal catalysis, in: B. Rieger, L.S. Baugh, S. Kacker, S. Striegler (Eds.), Late Transition Metal Polymerization Catalysis, WILEY-VCH Verlag, Weinheim, 2003, pp. 101–154.

[20] S. Hayakawa, H. Burgoon, J.A. Niemiec, D. Skilskyj, L.F. Rhodes; Promerus LLC. Palladium Catalysts for Forming Vinyl Addition Polymers Having Improved Film Forming Properties. U.S. Patent Pending.

[21] H. Masunaga, H. Ogawa, T. Takano, S. Sasaki, S. Goto, T. Tanaka, T. Seike, S. Takahashi, K. Takeshita, N. Nariyama, H. Ohashi, T. Ohata, Y. Furukawa, T. Matsushita, Y. Ishizawa, N. Yagi, M. Takata, H. Kitamura, K. Sakurai, K. Tashiro, A. Takahara, Y. Amamiya, K. Horie, M. Takenaka, T. Kanaya, H. Jinnai, H. Okuda, I. Akiba, I. Takahashi, K. Yamamoto, M. Hikosaka, S. Sakurai, Y. Shinohara, A. Okada, Y. Sugihara, Multipurpose soft-material SAXS/WAXS/GISAXS beamline at SPring-8, Polym. J. 43 (2011) 471–477, https://doi.org/10.1038/pj.2011.18.

[22] A. Takahara, T. Takeda, T. Kanaya, N. Kido, K. Sakurai, H. Masunaga, H. Ogawa, M. Takata, Advanced soft material beamline consortium at SPring-8 (FSBL), Synchrotron Radiat. News 27 (2014) 19–23, https://doi.org/10.1080/08940886.2014.908759.

[23] T.F.A. Haselwander, W. Heitz, M. Maskos, Vinylic polymerization of norbornene by Pd(II)-catalysis in the presence of ethylene, Macromol. Rapid Commun. 18 (1997) 689–697, https://doi.org/10.1002/marc.1997.030180810.

[24] K. Müller, S. Kreiling, K. Dehnicke, J. Allgaier, D. Richter, L.J. Fetters, Y. Jung, D. Y. Yoon, A. Greiner, Synthesis and rheological properties of poly(5-n-hexylnorbornene), Macromol. Chem. Phys. 207 (2006) 193–200, https://doi.org/10.1002/macp.200500228.

[25] B.G. Shin, T.Y. Cho, D.Y. Yoon, B. Liu, Structure and properties of polynorbornene derivatives: poly(norbornene dicarboxylic acid dialkyl ester)s and poly(norbornene dimethyl dicarboxylate)s, Macromol. Res. 15 (2007) 185–190, https://doi.org/10.1007/BF03218772.

[26] S.V. Mulpuri, J. Shin, B.G. Shin, A. Greiner, D.Y. Yoon, Synthesis and characterization of substituted polynorbornene derivatives, Polymer 52 (2011) 4377–4386, https://doi.org/10.1016/j.polymer.2011.07.019.